

# Limits on diffuse fluxes of high energy extraterrestrial neutrinos with the AMANDA-B10 detector

J. Ahrens<sup>12</sup>, X. Bai<sup>1</sup>, S. W. Barwick<sup>6</sup>, R. C. Bay<sup>5</sup>, T. Becka<sup>12</sup>, K.-H. Becker<sup>13</sup>, E. Bernardini<sup>2</sup>, D. Bertrand<sup>10</sup>, A. Biron<sup>2</sup>, S. Boeser<sup>2</sup>, O. Botner<sup>11</sup>, A. Bouchta<sup>11</sup>, O. Bouhali<sup>10</sup>, T. Burgess<sup>4</sup>, S. Carius<sup>3</sup>, T. Castermans<sup>16</sup>, D. Chirkin<sup>5</sup>, J. Conrad<sup>11</sup>, J. Cooley<sup>8</sup>, D. F. Cowen<sup>7</sup>, A. Davour<sup>11</sup>, C. De Clercq<sup>15</sup>, T. DeYoung<sup>8</sup>, P. Desiati<sup>8</sup>, P. Doksus<sup>8</sup>, P. Ekström<sup>4</sup>, T. Feser<sup>12</sup>, T. K. Gaisser<sup>1</sup>, R. Ganugapati<sup>8</sup>, M. Gaug<sup>2</sup>, H. Geenen<sup>13</sup>, L. Gerhardt<sup>6</sup>, A. Goldschmidt<sup>9</sup>, A. Hallgren<sup>11</sup>, F. Halzen<sup>8</sup>, K. Hanson<sup>8</sup>, R. Hardtke<sup>8</sup>, T. Hauschildt<sup>2</sup>, M. Hellwig<sup>12</sup>, P. Herquet<sup>16</sup>, G. C. Hill<sup>8</sup>, P. O. Hulth<sup>4</sup>, B. Hughey<sup>8</sup>, K. Hultqvist<sup>4</sup>, S. Hundertmark<sup>4</sup>, J. Jacobsen<sup>9</sup>, A. Karle<sup>8</sup>, K. Kuehn<sup>6</sup>, J. Kim<sup>6</sup>, L. Köpke<sup>12</sup>, M. Kowalski<sup>2</sup>, J. I. Lamoureux<sup>9</sup>, H. Leich<sup>2</sup>, M. Leuthold<sup>2</sup>, P. Lindahl<sup>3</sup>, I. Liubarsky<sup>18</sup>, J. Madsen<sup>14</sup>, K. Mandli<sup>8</sup>, P. Marciniowski<sup>11</sup>, H. Matis<sup>9</sup>, C. P. McParland<sup>9</sup>, T. Messarius<sup>13</sup>, T. C. Miller<sup>1</sup>, Y. Minaeva<sup>4</sup>, P. Miocinović<sup>5</sup>, P. C. Mock<sup>6</sup>, R. Morse<sup>8</sup>, T. Neunhoffer<sup>12</sup>, P. Niessen<sup>15</sup>, D. R. Nygren<sup>9</sup>, H. Ögelman<sup>8</sup>, P. Olbrechts<sup>15</sup>, C. Pérez de los Heros<sup>11</sup>, A. C. Pohl<sup>3</sup>, R. Porrata<sup>6</sup>, P. B. Price<sup>5</sup>, G. T. Przybylski<sup>6</sup>, K. Rawlins<sup>8</sup>, E. Resconi<sup>2</sup>, W. Rhode<sup>13</sup>, M. Ribordy<sup>2</sup>, S. Richter<sup>8</sup>, J. Rodríguez Martino<sup>4</sup>, P. Romenesko<sup>8</sup>, D. Ross<sup>6</sup>, H.-G. Sander<sup>12</sup>, S. Schlenstedt<sup>2</sup>, K. Schinarakis<sup>13</sup>, T. Schmidt<sup>2</sup>, D. Schneider<sup>8</sup>, R. Schwarz<sup>8</sup>, A. Silvestri<sup>6</sup>, M. Solarz<sup>5</sup>, M. Stamatikos<sup>8</sup>, G. M. Spiczak<sup>14</sup>, C. Spiering<sup>2</sup>, D. Steele<sup>8</sup>, P. Steffen<sup>2</sup>, R. G. Stokstad<sup>9</sup>, K.-H. Sulanke<sup>2</sup>, I. Taboada<sup>17</sup>, S. Tilav<sup>1</sup>, W. Wagner<sup>13</sup>, C. Walck<sup>4</sup>, Y.-R. Wang<sup>8</sup>, C. H. Wiebusch<sup>2</sup>, C. Wiedemann<sup>4</sup>, R. Wischniewski<sup>2</sup>, H. Wissing<sup>2</sup>, K. Woschnagg<sup>5</sup>, W. Wu<sup>6</sup>, G. Yodh<sup>6</sup>, S. Young<sup>6</sup>

<sup>1</sup>*Bartol Research Institute, University of Delaware, Newark, DE 19716*

<sup>2</sup>*DESY-Zeuthen, D-15735, Zeuthen, Germany*

<sup>3</sup>*Dept. of Technology, University of Kalmar, S-39182, Kalmar, Sweden*

<sup>4</sup>*Department of Physics, Stockholm University, SE-106 91 Stockholm, Sweden*

<sup>5</sup>*Dept. of Physics, University of California, Berkeley, CA 94720*

<sup>6</sup>*Dept. of Physics and Astronomy, University of California, Irvine, CA 92697*

<sup>7</sup>*Dept. of Physics, Pennsylvania State University, University Park, PA 16802*

<sup>8</sup>*Dept. of Physics, University of Wisconsin, Madison, WI 53706*

<sup>9</sup>*Lawrence Berkeley National Laboratory, Berkeley, CA 94720*

<sup>10</sup>*Universite Libre de Bruxelles, Science Faculty CP230, Boulevard du Triomphe, B-1050, Brussels, Belgium*

<sup>11</sup>*Division of High Energy Physics, Uppsala University, S-75121, Uppsala, Sweden*

<sup>12</sup>*Institute of Physics, University of Mainz, Staudinger Weg 7, D-55099, Mainz, Germany*

<sup>13</sup>*Fachbereich 8 Physik, BUGH Wuppertal, D-42097 Wuppertal Germany*

<sup>14</sup>*Physics Dept., University of Wisconsin, River Falls, WI 54022*

<sup>15</sup>*Vrije Universiteit Brussel, Dienst ELEM, B-1050, Brussels, Belgium*

<sup>16</sup>*Université de Mons-Hainaut, 19 Avenue Maistriau 7000, Mons, Belgium*

<sup>17</sup>*Dept. Física, University Simón Bolívar, Caracas, Venezuela and*

<sup>18</sup>*Blackett Laboratory, Imperial College, London SW7 2BW, United Kingdom*

Data from the AMANDA-B10 detector taken during the austral winter of 1997 have been searched for a diffuse flux of high energy extraterrestrial muon-neutrinos, as predicted from, e.g., the sum of all active galaxies in the universe. This search yielded no excess events above those expected from the background atmospheric neutrinos, leading to upper limits on the extraterrestrial neutrino flux. For an assumed  $E^{-2}$  spectrum, a 90% classical confidence level upper limit has been placed at a level  $E^2\Phi(E) = 8.4 \times 10^{-7} \text{ cm}^{-2} \text{ s}^{-1} \text{ sr}^{-1} \text{ GeV}$ , (for a predominant neutrino energy range 6-1000 TeV) which is the most restrictive bound placed by any neutrino detector. When specific predicted spectral forms are considered, it is found that some are excluded.

PACS numbers: 95.55.Vj, 95.85.Ry, 96.40.Tv, 98.54.-h

High energy extraterrestrial neutrinos are believed to be produced in energetic accelerated environments through proton-proton or proton-photon interactions via pion production and decay. Such an accelerator might be the core of an active galaxy, powered by a supermassive black hole. In their pioneering work, Stecker, Done, Salamon and Sommers [1] calculated the expected diffuse flux of neutrinos from the sum of all active galaxies and

found that such a flux could be observable deep underground in a large neutrino detector. Further predictions have followed (for a summary see for example the review of Learned and Mannheim [2]), and with the construction and operation of the first high energy neutrino detectors, the sensitivity has been reached to enable such predictions to be tested. Searches have been made and limits have been reported by the DUMAND [3], Frejus

[4], Baikal( $\nu_e$ ) [5, 6], MACRO [7] and AMANDA( $\nu_e$ ) [8] neutrino detectors. In this letter, we describe the search for high energy extraterrestrial neutrino-induced muons, using data collected during the austral winter of 1997 with the AMANDA-B10 detector [9, 10], located in the antarctic ice cap at the South Pole station.

The AMANDA (Antarctic Muon And Neutrino Detector Array) telescope detects high-energy muon-neutrinos by observing Cherenkov light from muons resulting from neutrino interactions in the ice surrounding, or the rock, below the detector. While extraterrestrial neutrinos will produce high-energy muons from all arrival directions, those coming from *above* the detector will be very difficult to separate from the overwhelming flux of downward-going cosmic-ray induced atmospheric muons. The majority of these muons are rejected by only accepting upward going neutrino-induced muons; the earth filters out muons produced in the atmosphere on the other side of the planet. There is a small remaining flux of misreconstructed events which is removed by quality cuts that leave only well reconstructed events. After the atmospheric muons are removed, there will remain a flux of upward going muons from cosmic ray induced atmospheric neutrinos that have penetrated the earth and interacted near the detector. This relatively well understood neutrino flux is a background to the search but has been used to verify the performance of the detector [9, 10]. The separation of the extraterrestrial neutrino-induced muons from the atmospheric neutrino-induced muons is based on the expected energy spectrum of the detected muons. Typically, a model of an extraterrestrial source of neutrinos has a harder spectrum (e.g.  $\sim E^{-2}$ ) [11] than that of the atmospheric neutrinos ( $\sim E^{-3.7}$ ) [12, 13]. After accounting for neutrino interaction and muon propagation, this energy difference carries over to produce a harder muon energy spectrum for the extraterrestrial neutrino-induced muons near the detector. The energy of the muon is not measured directly, but more energetic muons tend to produce more Cherenkov light and thus more hit optical modules in the detector, and this observable, the channel multiplicity ( $N_{\text{ch}}$ ), is used as the primary separator of higher energy extraterrestrial neutrino-induced muon events from the background of lower energy atmospheric neutrino-induced muons.

In this analysis, the event selection cuts were designed to retain high energy track-like events [14]. The detector simulation has changed from that used in the atmospheric neutrino analysis [10]. A new muon propagation code [15] was used, which accounts for all relevant stochastic light emission from the muons. The depth-dependent optical properties of the fiducial ice were determined using atmospheric muons as a calibration source.

Before the energy sensitive channel multiplicity cut was finally applied, 69 events remained in the data sample, whereas a full simulation of the detector response to the

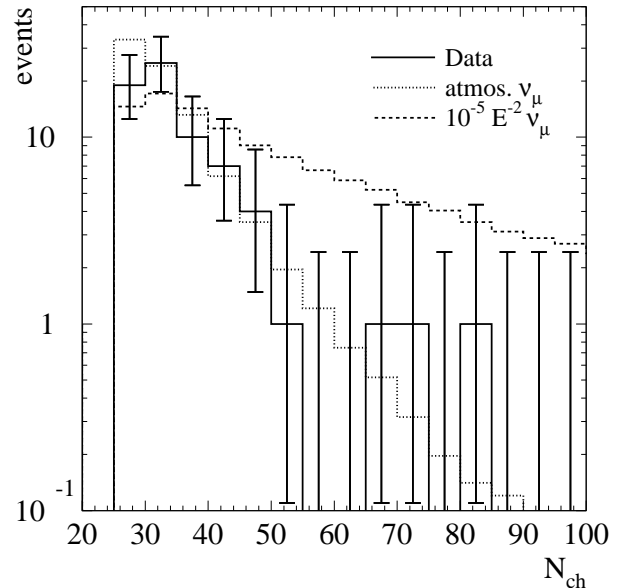


FIG. 1: Channel multiplicity distribution after final cuts, showing the expected excess of events from an  $E^{-2}$  spectrum at the higher multiplicities.

atmospheric neutrino (Lipari [12]) flux (neglecting neutrino oscillations, which would reduce the prediction by only a few percent) predicts 85 events for the 130 days of live time. The absolute difference in the numbers of events is consistent with Poisson fluctuations, or with the  $\pm 25\%$  [13] uncertainty in the atmospheric neutrino flux, or with uncertainties in the simulation efficiencies. The distribution of the data and atmospheric simulation are shown in figure 1. The error bars on the data are 90% unified confidence intervals [16] for the fixed but unknown value of the mean rate  $\mu = \mu_b + \mu_s$  for each bin. Only one bin ( $N_{\text{ch}} = 25 - 30$ ) has a background prediction inconsistent with the confidence interval. More specifically, a generalised likelihood ratio test of the shape of the atmospheric neutrino hypothesis as the parent distribution of the data yields a chance probability of 20%, which is too large to reject the shape of the atmospheric neutrino hypothesis. We choose to treat the rate of observed atmospheric neutrinos as a constraint on the overall detector efficiency and then carry through an efficiency uncertainty from the atmospheric neutrino flux prediction and Poisson error on the observed rate. Therefore, to calibrate the overall detector sensitivity, we take the 69 events as the best-fit estimate of the number of atmospheric neutrinos and rescale all efficiencies by a factor 69/85. This is conservative, since if the first bin discrepancy was due e.g. to a simulation effect, then no renormalisation would be needed, and the limits would

improve slightly. We combine the Poisson error on the observed rate of atmospheric neutrinos with the theoretical flux uncertainty (taken as a uniform probability distribution centred about the best-fit flux  $\hat{\Phi}$  and extending to  $\pm 0.25\hat{\Phi}$ ) to compute the correlations between the background and efficiency for later use in the probability distribution function used in the confidence interval construction. To incorporate these systematic uncertainties in the efficiencies into the limit calculations, we follow the prescription of Cousins and Highland [17], as implemented by Conrad *et al.* [18] with the unified Feldman-Cousins ordering and improved by a more appropriate choice of the likelihood ratio test [19]. We also report all limits and sensitivities with and without the assumed uncertainty.

In addition to the data and atmospheric neutrino prediction, figure 1 also shows the prediction for an  $E^{-2}$  signal flux at a level  $E^2\Phi(E) = 10^{-5} \text{ cm}^{-2} \text{ s}^{-1} \text{ sr}^{-1} \text{ GeV}$ , a flux that would have been readily detected. Setting a limit on a flux  $\Phi(E)$  involves determining an experimental signal event upper limit  $\mu(n_{\text{obs}}, n_{\text{b}})$ , which is a function of the number of observed events,  $n_{\text{obs}}$ , and expected background,  $n_{\text{b}}$ , after the cuts are applied. A simulation chain accounting for neutrino absorption, interaction and neutral current regeneration, muon propagation and detector response gives the number of signal events,  $n_{\text{s}}$ , expected from the source flux  $\Phi(E)$ . The limit on the source flux will then be  $\Phi_{\text{limit}}(E) = \Phi(E) \times \mu(n_{\text{obs}}, n_{\text{b}}) / n_{\text{s}}$ . The choice of final cut is optimised before examining the data by minimising the average “model rejection factor” (MRF)  $\bar{\mu}(n_{\text{obs}}, n_{\text{b}}) / n_{\text{s}}$  [20], where the as yet unknown experimental event limit  $\mu(n_{\text{obs}}, n_{\text{b}})$  is replaced by the *average* upper limit  $\bar{\mu}(n_{\text{b}})$  [16]. Over an ensemble of hypothetical repetitions of the experiment, this choice of cut will lead to the best average limit  $\bar{\Phi}_{\text{limit}}(E)$ .

The integrated channel multiplicity distribution is shown in figure 2. Also shown is the 90% confidence level Feldman-Cousins average upper limit which is a function of the expected background. The optimal cut is the one where the model rejection factor  $\mu(n_{\text{b}}) / n_{\text{s}}$  is minimised. Figure 2 also shows the average flux upper limit ( $E^2\Phi \times \text{MRF}$ ) as a function of the choice of multiplicity cut. The minimum flux limit occurs at a cut of  $N_{\text{ch}} \geq 54$ , where we expect  $n_{\text{b}} = 3.06$  and an average signal event upper limit of 4.43 ignoring the uncertainties in the efficiency and background, and 4.93 when the uncertainties are included. The  $10^{-5}E^{-2}$  signal flux would produce 56.7 events. This leads to corresponding expected average limits on the source flux of  $E^2\bar{\Phi}_{90\%}(E) = 7.8 \times 10^{-7} \text{ cm}^{-2} \text{ s}^{-1} \text{ sr}^{-1} \text{ GeV}$  (excluding uncertainties), and  $8.7 \times 10^{-7} \text{ cm}^{-2} \text{ s}^{-1} \text{ sr}^{-1} \text{ GeV}$  (including uncertainties).

We note that the expected overall flux limit is relatively insensitive to the choice of cut, with a broad minimum seen in figure 2 in the range of multiplicities 50-70. We now apply this optimal multiplicity cut to the data,

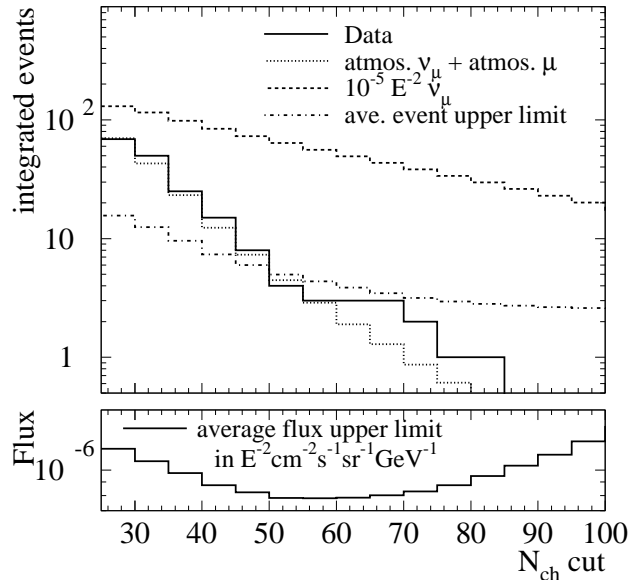


FIG. 2: Integrated distributions of event numbers as a function of the multiplicity cut (top plot). The minimum in the flux average upper limit (bottom) is found by minimising the ratio of the average event upper limit to the expected  $E^{-2}$  signal.

and find that 3 events remain. Ignoring the systematic uncertainties gives an event limit of 4.36 and a flux upper limit of  $E^2\Phi_{90\%}(E) = 7.7 \times 10^{-7} \text{ cm}^{-2} \text{ s}^{-1} \text{ sr}^{-1} \text{ GeV}$ . Including the systematic uncertainties leads to an event limit of 4.75 and our final flux limit on an  $E^{-2}$  spectrum of  $E^2\Phi_{90\%}(E) = 8.4 \times 10^{-7} \text{ cm}^{-2} \text{ s}^{-1} \text{ sr}^{-1} \text{ GeV}$ .

Figure 3 shows the neutrino energy spectrum of the simulated events before and after the multiplicity cut of 54 channels, for both atmospheric neutrinos and neutrinos from an  $E^{-2}$  spectrum. The multiplicity cut corresponds to a sensitive energy range of 6-1000 TeV, which contains 90% of the expected  $E^{-2}$  signal. The peak response energy is just below 100 TeV.

Just as a limit was placed on an assumed  $E^{-2}$  spectrum, limits can be placed on any neutrino flux prediction, and we consider a sample of predictions that are near the limit-setting capability of the detector (MRF  $\sim 1$ ). For each case, we optimise the final  $N_{\text{ch}}$  cut to minimise the expected average flux upper limit, then compare the expected number of extraterrestrial neutrino events after the cuts to the observed event limit; those predictions that produce expected event numbers greater than the observed event limit are excluded at the stated classical confidence level. The results of these calculations are shown in table I and in figure 4. For each flux we again report two sensitivities and limits - one assuming no systematic uncertainties and the second including

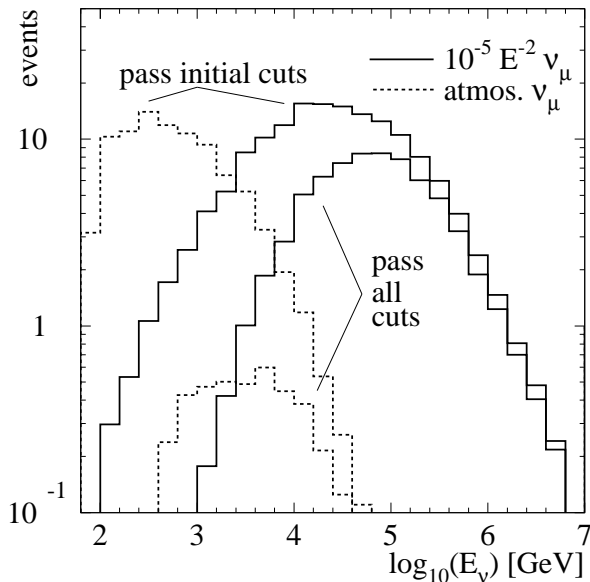


FIG. 3: Energy spectrum of the incident atmospheric (dashed lines) and  $E^{-2}$  (solid lines) neutrinos for events that pass the initial cuts (thin lines), and have channel multiplicity greater than the optimum cut of 54 channels (thick lines).

systematic uncertainties. We find that the predictions of Szabo and Protheroe (SPH92L [21], P96p $\gamma$ pp [22]) are excluded. The quasar core (SSQC) prediction of Stecker and Salamon [11] is just excluded (MRF = 0.98), but the blazar jet (SSBJ) prediction is not. The limit of the original Stecker, Done, Salamon and Sommers flux [1] (SDSS) is a factor of 2 above the prediction and therefore the prediction is not excluded.

Maximal mixing from neutrino oscillations [23, 24] between  $\nu_\mu$  and  $\nu_\tau$  during propagation to the earth would lead to limits a factor of two greater than quoted here due to the loss of half the expected  $\nu_\mu$  flux into the  $\nu_\tau$  state. However, some of these  $\nu_\tau$  would regenerate  $\nu_\mu$  in the earth ( $\nu_\tau \rightarrow \tau \rightarrow \nu_\mu$ ) lessening the effect [25, 26].

We also place a limit on a model of prompt charm induced neutrinos [27] (ZHV92) in the earth's atmosphere and find that the detector sensitivity is about a factor of 4 away from excluding the prediction. More recent predictions are even further below the sensitivity of the detector [28].

Since most events will originate from neutrinos near the peak of the detector sensitivity  $E_\nu \sim 10^5$  GeV, the limits at that point for the three different spectral shapes ( $E^{-2}$ , SSQC and Charm D) are similar, as seen in figure 4.

The limits presented in this letter, based on the first real-time year of operation of the AMANDA-B10 de-

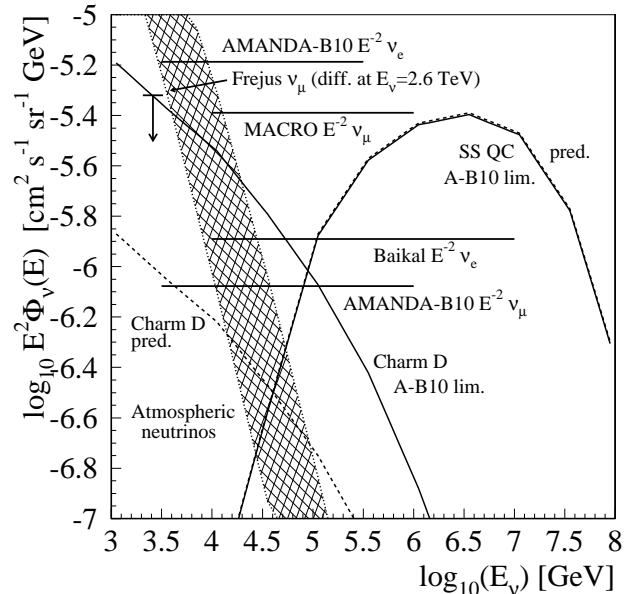


FIG. 4: Summary of experimental 90% classical confidence level flux limits from various detectors assuming an  $E^{-2}$  spectrum. From top: AMANDA-B10 ( $\nu_e$ ) [8], Frejus [4], MACRO [7], Baikal [6] and AMANDA-B10 ( $\nu_\mu$ ) (this work). The background atmospheric neutrinos [12] are indicated by the hashed region representing the angular dependence of the flux. Also shown are the predicted fluxes (dashed), and AMANDA-B10 experimental flux limits (solid) for a diffuse AGN prediction (SSQC [11] – nearly overlapping dotted and dashed curves – MRF = 0.98) and for one prediction of prompt charm neutrino production in the earth's atmosphere [27]. Since most events will originate from neutrinos near the peak of the detector sensitivity ( $E_\nu \sim 10^5$  GeV), the limits at that point for different spectral shapes are similar.

tector, are the strongest placed to date on extraterrestrial diffuse neutrino fluxes. Since that year, we estimate that about 10 times the exposure has been achieved in total with AMANDA-B10 (1997-99) and the expanded AMANDA-II detector (2000-present). We anticipate this combined data set to have a limit-setting potential more than three times better than the results presented here.

We acknowledge the support of the following agencies: National Science Foundation–Office of Polar Programs, National Science Foundation–Physics Division, University of Wisconsin Alumni Research Foundation, Department of Energy, and National Energy Research Scientific Computing Center (supported by the Office of Energy Research of the Department of Energy), UC-Irvine AE-NEAS Supercomputer Facility, USA; Swedish Research Council, Swedish Polar Research Secretariat, and Knut and Alice Wallenberg Foundation, Sweden; German Ministry for Education and Research, Deutsche Forschungsgemeinschaft (DFG), Germany; Fund for Scientific Re-

TABLE I: Flux limits calculated for individual models of diffuse neutrino emission. The optimal  $N_{\text{ch}}$  cut, expected background and signal for each model are shown. The average upper limit ( $\bar{\mu}(n_b)$ ) and average model rejection factor ( $\bar{\mu}(n_b)/n_s$ ) are shown with and without the inclusion of systematic uncertainties. Finally the experimental limits (event limit  $\mu_o \equiv \mu(n_o, n_b)$ ) and model rejection factor ( $\mu_o/n_s$ ) are given for both systematic uncertainty assumptions.

Flux	nch cut	Sensitivities						Experimental limits					
		$n_b$	$n_s$	No sys. uncer.		Sys. uncer. inc.		No sys. uncer.		Sys. uncer. inc.			
				$\bar{\mu}(n_b)$	$\frac{\bar{\mu}(n_b)}{n_s}$	$\bar{\mu}(n_b)$	$\frac{\bar{\mu}(n_b)}{n_s}$	$n_o$	$\mu_o$	$\frac{\mu_o}{n_s}$	$\mu_o$	$\frac{\mu_o}{n_s}$	
$10^{-6}\text{E}^{-2}$	54	3.06	5.67	4.43	0.781	4.93	0.869	3	4.36	0.769	4.75	0.838	
SDSS [1]	73	0.69	2.42	3.01	1.240	3.38	1.397	2	5.22	2.157	5.61	2.318	
SPH92L [21]	58	2.12	12.66	3.97	0.314	4.33	0.342	3	5.30	0.419	5.69	0.449	
SSQC [11]	71	0.80	5.59	3.11	0.556	3.45	0.617	2	5.11	0.914	5.50	0.984	
SSBJ [11]	57	2.36	4.29	4.13	0.963	4.50	1.049	3	5.06	1.179	5.45	1.270	
P96p $\gamma$ pp [22]	49	4.83	21.95	5.11	0.233	5.90	0.269	4	3.76	0.171	4.54	0.207	
ZHV Charm D [27]	41	10.9	2.58	6.97	2.702	8.42	3.264	14	10.60	4.109	12.31	4.771	

search (FNRS-FWO), Flanders Institute to encourage scientific and technological research in industry (IWT), and Belgian Federal Office for Scientific, Technical and Cultural affairs (OSTC), Belgium. D.F.C. acknowledges the support of the NSF CAREER program.

[1] F. W. Stecker, C. Done, M. H. Salamon and P. Sommers, Phys. Rev. Lett. **66** 2697 (1991), Errata, Phys. Rev. Lett. **69** 738 (1992).  
[2] J. G. Learned and K. Mannheim, Ann. Rev. Nucl. Part. Sci. **50** 679 (2000).  
[3] J. W. Bolesta, *et al.*, Proc. 25th Int. Cosmic Ray Conf. **7** 29 (1997).  
[4] W. Rhode *et al.*, Astropart. Phys. **4** 217 (1996).  
[5] V.A. Balkanov, *et al.*, Astropart. Phys. **14** 61 (2000).  
[6] Zh.-A. Dzhilkibaev *et al.*, Proc. Int. Conf. on Neutrino Telescopes, Venice astro-ph/0105269 (2001).  
[7] M. Ambrosio, *et al.*, Astropart. Phys. in press (2002).  
[8] J. Ahrens *et al.*, Phys. Rev. D **67** 012003 (2003).  
[9] E. Andrés, *et al.*, Nature **410** 441 (2001).  
[10] J. Ahrens *et al.*, Phys. Rev. D **66** 012005 (2002).  
[11] F. W. Stecker and M. H. Salamon, Space Sci. Rev. **75** 341-355 (1996).  
[12] P. Lipari, Astropart. Phys. **1** 195 (1993).  
[13] T. K. Gaisser and M. Honda, Ann. Rev. Nucl. Part. Sci.

**52** 153 (2002).  
[14] M. Leuthold, *Search for Cosmic High Energy Neutrinos with the AMANDA-B10 Detector*, PhD thesis, Humboldt University, Berlin (2001).  
[15] D. Chirkin and W. Rhode, Proc. 27th Int. Cosmic Ray Conf., HE 220, Hamburg, (2001).  
[16] G. J. Feldman and R. D. Cousins, Phys. Rev. D **57** 3873 (1998).  
[17] R. D. Cousins and V. L. Highland, Nucl. Ins. Meth. Phys. Res. **A320** 331 (1992).  
[18] J. Conrad *et al.*, Phys. Rev. D. **67** 012002 (2003).  
[19] G. C. Hill, Phys. Rev. D. submitted, (physics/0302057) (2003).  
[20] G. C. Hill and K. Rawlins, Astropart. Phys. in press, (astro-ph/0209350) (2003).  
[21] A. P. Szabo and R. J. Protheroe, Proc. Workshop on High Energy Neutrino Astronomy, page 24, University of Hawaii, World Scientific, (1992).  
[22] R. J. Protheroe, Proc. IAU Colloquium **163** 585 (1997).  
[23] Y. Fukuda *et al.*, Phys. Rev. Lett. **81** 1562 (1998).  
[24] Q. R. Ahmad *et al.*, Phys. Rev. Lett. **87** 071301 (2001).  
[25] F. Halzen and D. Saltzberg, Phys. Rev. Lett. **81** 4305 (1998).  
[26] J. F. Beacom, P. Crotty, and E. W. Kolb, Phys. Rev. D **66** 021302 (2002).  
[27] E. Zas, F. Halzen and R. A. Vázquez, Astropart. Phys. **1** 297 (1993).  
[28] C. G. S. Costa, Astropart. Phys. **16** 193 (2001).